In-Process Machine Vision by Mono-Electron Image Acquisition and Analysis under Scale-Up Nano-Manufacturing Conditions

E. E. Jumbo[1], K. Kotingo[1], T. E. Isaiah[1], A. N. Okpala[1], N. Olali[2]

[1] *Department of Mechanical and Marine Engineering, Niger Delta University*
[2] *Department of Mathematics and Computer Science, Niger Delta University*
Corresponding author: E. E. Jumbo

Abstract: *Manufacturing process automation have attained significant progress by the incorporation of AI and many other forms of machine vision technologies. In this paper, the stoichiometric dynamics relative to image acquisition and interpretation under nanoscale manufacturing conditions have been discussed and theoretically analyzed using relevant space and state predictive simulations. It was shown that the in-process manufacturing conditions incidental to this image analysis utilized process invariant criticalities bothering on Bohr and Bolztmann's postulations. Thus, this imaging possibility was further shown to be dependent on the structural conditions and orientation of an electron in addition to its femtoseconds' time constraint situation for target surface image acquisition and analysis. Further, this investigation indicate the opto-electromechanical cavity realities of the photonic-phononic scanning electron relativities.*

Keywords: *particulate, optimization, undulator, trajectory, photonic-phononic*

I. Introduction

Nanoscale manufacturing is a product realizable scientific imagination that deals with matter at infinitesimally minute conditions of existence. Thus, *nano-manfacturing* deals with the control and physical simulation of intangible matter. This approach to advanced manufacturing capabilities holds significant relevance to miniaturized manufacture conditions that are nanoscale in nature.

Secondly, modern scientific evolution has also drawn attention to visualization and in-service control of process sequences during material treatment and combinations at atomic and molecular scale. Consequently, this paper shall review and advance the existing technologies of x-ray free-electron laser applications in high speed process acquisition sequence and manufacturing conditions. Since the application of x-ray FEL have gained tremendous attention in medical, and environmentally hazardous conditions.

In view of the foregoing an integration of x-ray FEL into any manufacturing strategy increases the output per investment and guarantees high quantity and product precision and predictability. The reasons for these anticipations are x-ray FELs characteristic qualities of tunability, coherence, significant high peak power in addition to a relatively short pulse length. It should be noted that the suitability of x-ray FELs for this application is significantly dependent on its capability to explore any given mass or particulate matter at the dimensions and time invariants akin to microscopic conditions of atomic and molecular relativity. Thus, structurally the Bohr atomic radius measuring about 1Å defines approximately the size orientation in phenomenal space of the trajected electron which takes *Bohrs* period of 1 femtosecond in relation to the decapitulation or harvesting of a valence electron. Further, since electrons themselves are trajected alongside electromagnetic radiation and light emission, it is imperative to note that the particulate nature of electrons also makes them capable of *particulate orientations* and characteristics.

1.1   Mechanics of Free-Electron Laser Technology

In view of modern technologically driven manufacturing initiatives, high sequence manufacturing output is a direct offshoot of manufacturing process optimizations that are dependent on advancements in engineering materials processing technologies. Thus, a healthy combination of these materials results better products initiatives. Pursuant to the foregoing, the proposition of this paper with respect to high speed manufacturing up-scale machine vision and communication is timely; especially in the arena of high precision in-process manufacturing automation conditions. Thus, the advancement in the integration of machine vision technology within atomic, molecular and nanoscale dimension is a crucial emerging technological and scientific innovation, as would be seen in the sections that follow.

1.2 Electron Cloud Saturation Mechanics and Directional Dynamics

Consider an electron in a characteristic field created by wriggle magnetic field consisting of opposing poles magnets as demonstrated below;
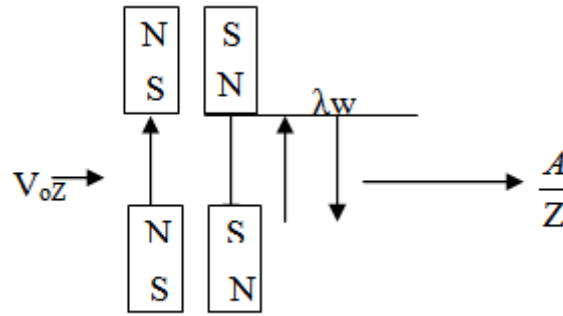
Fig 1: Wriggle effect magnetic field

The Fig. 1 above indicate mono-electron mobility situation under wriggle magnetic field and the structural conditions of a unit of undulating magnetic system where the magnetic field characteristics are defined by the equation;

$$B\omega = A_w e^{ikwz} \tag{1}$$

where $kw = 2\pi / \lambda w$ and field potentials is an oscillatory transverse to the positive direction of electron propagation.

Structurally, the energy possessed by this electron is affected or influenced by the magnetic field of a specified period, Δw (in cm) which is sinusoidal in nature and defined by amplitude $B\omega$, (in Tesla) as indicated in equation (1) above.

II. Mono-Electron Computational Analysis

In view of the foregoing, consider an electron in an electron beam traversing the undulator and trajected by wave train expressed as μ_w at a wave dimensional condition of;

$$\lambda = \lambda_w (1 + K^2 + \gamma^2\theta^2)/2\gamma^2 \tag{2}$$

On the condition of *electron material transportation impact index trajectory*, $e_{i(n)}$, equation (2) becomes;

$$\lambda_{i(n)} = \lambda_{wi(n)}(1 + K^2 + \gamma^2\theta^2)/2\gamma^2 \tag{3}$$

Thus equation (3) defines a complicated structural transformation of the single electron where the $i_{(n)}$ component expresses the totality of the intended impact of the beam. In equation (3), γ is the cumulative beam energy contributed by the individual electrons, while θ is the assignable angle between the undulator dimensional axis and the observable radiation line of sight from the point of an observer. The *K* factor defines the active undulator parametric effect on the electron and is relatively expresses as; $K = eB_w\lambda_w/2\pi MC^2$. It should be pointed that where planar undulators are used, the formula for the parametric *K-factor* will also be adapted to suit the particular modification[1]. Implying that the line width of $\Delta\lambda/\lambda = 1/\mu_w$ is appropriate.

Further, it should be noted that the wavelength generated by this single electron trajectory is directly dependent on the angular orientation of the electron[1], thus, initiating and sustaining the idea of a unified or coherent angle which studies have indicated is in tandem with the line width, $\Delta\lambda/\lambda = \mu_w^{-1}$. Thus, coherent angle bordering on this line width impliedly suggest that the material transportation impact (MTI) also follows the trajectory producing the stated angle and can be expressed as;

$$\theta_{ic} = \left(\lambda/\lambda_{wi}\mu_{wi} = \mu_{wi}\right)^{1/2} \tag{4}$$

In view of the foregoing, it should be noted that this single electron trajectory of θ_{ic} characteristics, produces a diffraction source radius that is limited to the process constraint undulation within the range $\theta > 0 \leq \theta_{ic}$, where θ_{ic} defines the maximum boundary conditions of the material transportation impact

index in view of other components of the electron material transportation $e_{i(n)}$. In this case, the coherent angle source radius space containment is expressed as;

$$r_c = \left(\lambda \lambda_{wi} \mu_{wi}\right)^{1/2} \tag{5}$$

Instructively, the consequential impact of the surrounding conditions on the electron arising from the cumulative effect of the process constraints defined by equations (4) and (5) implies that;

$$\theta_{ic} r_c = \lambda / 4\pi \tag{6}$$

Thus, a graphical representation of this solid coherent angle and the source radius based on the trajectory of this single electron as expressed in equation (6) results opposing sides center end with 90° perpendicular projection as shown in Fig. 1 above.

In order to simulate the behavior of this particle in space, Marple Release 15 Solid Modeling and Processing Software was deployed. In view of this application, let $\mu = \theta_{ic}$ (which expresses the material transportation impact index (MTIi) and let $y = r_c$, (which refers to the solid space boundary condition). Further, let $\theta_{ic} r_c = z = \lambda / 4\pi$, then the possibility of a 3-D simulation of the process constraints defined by z $= \lambda / 4\pi$ would be assumed to completely exist along the *z-axis* where $\lambda = x$ and $4\pi = y$. Thus, z = $\dfrac{x}{y}$, within the containment of available space.

In addition to the foregoing suppositions and given that the mass of an electron[2] is 9.109 x 10^{-31} kg, electron potential eV = 1.6022 x 10^{-19} (1 *eV* being the work of a charge *e* of 1 electron carried through a potential difference 1 volt) [2] and Plank's Constant, $\hbar = 6.626 x 10^{-34} J - s$, the wavelength λ of an electron thus becomes;

$$\lambda = \frac{\hbar}{\sqrt{2meV}} \tag{7}$$

Further, it has been reported that experimental results using scanning electron microscope (SEM) revealed that electron velocities attain about 70 of the speed of light when accelerating voltage of 200KeV is applied.[3] This discussion posits that under such application certain changes in electron mobility orientations are bound to be affected. These includes length squeezing or contraction, time dilation and increase in electron mass.

Under mono-electron potentiation, these differences are taken into account resulting the wavelength expressed in equation (8) below:

$$\lambda = \frac{12.25 x 10^{-10}}{\sqrt{V}} * \frac{1}{\sqrt{1 + \dfrac{eV}{2mc^2}}} \tag{8}$$

Where *c* is the speed of light given as 3 x 10^8m/s, the wavelength of an electron upon computation of the above yields the results stated in the following table which is based on scanning electron microscope simulation experiment:

Table 1- Experimental readings from SEM

Experiment	Electron potential (eV)	Electron Wavelength (λm)
1	10	12.2
2	100	3.70
3	200	2.51
4	300	1.96

Thus, Table 1 can further be analyzed as indicated in Fig. 2 below. The structural orientation of electron mass mobility towards the target point is indicated to show rise in the quantity and quality of electron wavelength due to increase in electron voltage, required to liberate and traject electrons into the conduction and valence band. In view of this finding, in should be noted that as potential voltage increases the value of eV output, wavelength reduces and becomes shorter and intensified. These intensified wavelengths imply higher impacts on the scan target.

Experimental reading from SCM sequence simulation
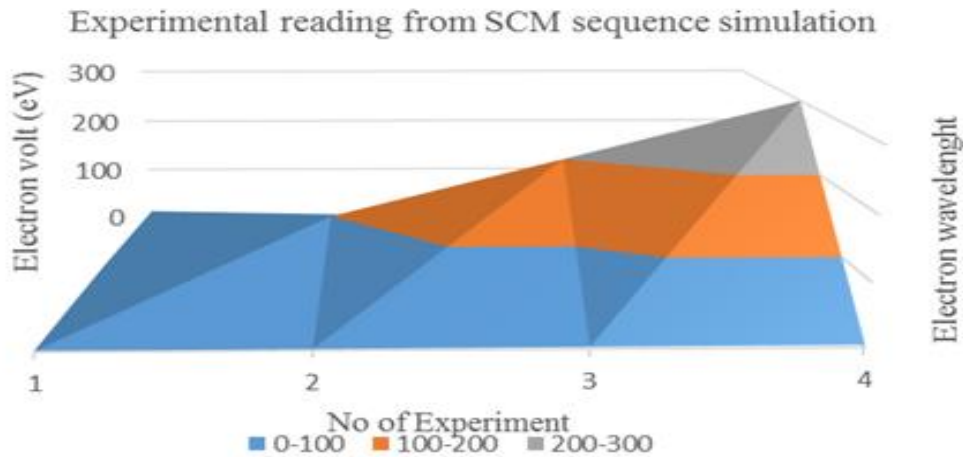
Fig 2: 3-D graph of the experimental reading from SEM sequence simulation in relation to electron emission in wavelength (λm) as corresponding excitation or electron volt, eV. The graph indicates electron migration tendency from the conduction band towards the scan target. Although in 3-D presentation the graph above is a 359.9° rotational skew akin to a 4-D solid demonstration indicating a sharp point of impact of the single electron on the target in order to be imparted with the structural characteristics of the surface.
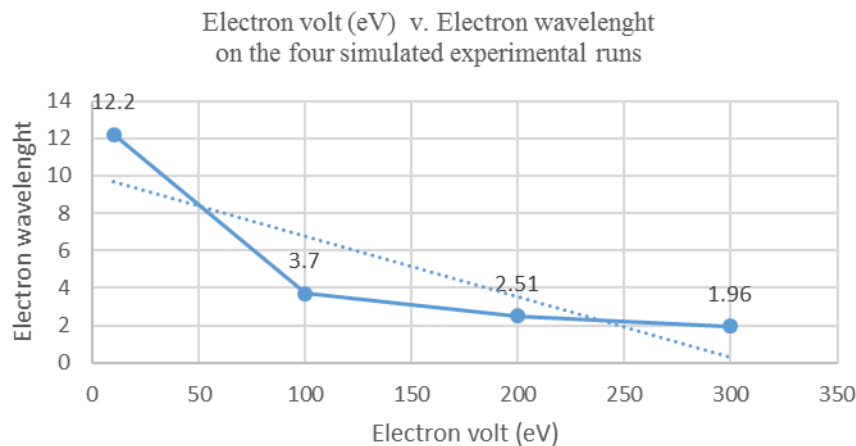
Fig 3: graph of electron volt v. electron wavelength indicating decrease in electron wavelength as electron volt increases. Implying increase in emission and trajectory force upon increase in electron volt. This increase in wavelength also indicate significant rise in intensity due to reduced amplitude in the waveform.

III. Mechanics Of Photonic-Photonic Coherency In Scanning Beam Propagation

The discussion above borders on one electron material transportation impact index, indicating that electron induced photonic emission also jointly propagate with its phononic components [3, 4]. Accordingly, studies have shown that a phonon is a definite discrete unit or quantum of vibrational mechanical energy.[4] In view of this vibrational phenomena, it should be noted that a phonon is the vibrational motion provider that accompanies an electron when atomic energy level instability results emissions of photons.

Instructively, the photonic-phononic interactions were shown to be possible in the cavity optomechanics experiment[3] where there was a successful isolation, transmittal and coupling of optical and mechanical waves at nanoscale dimensions. Thus, the nanofabrication presented in that work support the establishment of cavity optomechanics [5] and also agrees with the view that phonons can be manipulated by various transducer applications [6] such as in remote sensing and terrestrial communications) to traverse through light. This implies a photonic sequence that supports mechanical vibrations as distinct quantized energy.

The relevance of the foregoing findings to this paper is the mechanics of the *trasndcutive enablement of light particles*, (photons) propagated and transmitted by mechanical vibrations (phonons) in such an admixture of optomechancial process sequence, logical enough to capture or receive images as defined quantities and relay

same for interpretations. Thus, a one electron, image acquisition process as exemplified in the SEM/FEL technology deployment in object oriented structural definitions draw inference from an electron beam image capturing situation where electrons are found to migrate in a random multilaterally longitudinal orientation. These electrons flow in sequence of wave phases randomly interposing and superimposing on each other with electron density per defined unit determining the physical and theoretical intensity of the beam, under this image acquisition and interpretation, an emitted electron/photon for this assignment must on the average form a defined streamline trajectory being product of coherent solid angles and trajectory phase determined by the relation,

$$N_{ph} = \pi\alpha k^2 /(1+k^2) \quad \sim 0.01 \tag{9}$$

where α is the structural constant definitive of the regularity of the electron/phonon size and *k* has been established [7] to be equal to $eB_w\lambda_w/2\pi mc^2$ which represents the undulator field parameter.

Thus, irrespective of equation (8) and the defined *k-factor*, the resulting idea that photonic trajectory coherency from an emitted electron is not mathematically feasible on account of the wave particle quantum regime. This view is of a theoretical relevance on account of unstable wave propagation dynamics. Thus, under single electron imagery condition, process coherency is most likely unachievable; except parameter redefinition for high electron excitation modulation under nanoscale conditions are optimized. It has therefore been suggested [8] that a single approach ideology to this novel area of science and its application, depends on the integration of total energy U_t of the aggregate coherent photons in a non-linearized x-ray condition. The result of this approach can further be treated under a single electron regime.

In view of the foregoing this section shall explore the impact of force fields on an electron's imaging capability. A careful consideration of an electron trajected in an undulator would indicate that the electron undergo a transition influenced by both magnetic and electric fields in the form of electromagnetic waves. [9]
The process characteristics of this waveform is defined by two wave components which can be stated as;

$$E_R = xE_R \, Cos \, (K_R Z - \omega_{Rt} + \emptyset_R) \tag{10}$$

and

$$B_R = yB_R \, Cos \, (K_R Z - \omega_{Rt} + \emptyset_R) \tag{11}$$

The foregoing implies that the electric field component of the wave form is defined by equation (10) which has a radiation frequency of $fR = 2\pi/\omega R$ with a vector consequence of $K_R = 2\pi/\lambda_R$. Theoretically, the λ_R component defines the wave input of the radiation emitted under the condition that the $\emptyset_R$ factor is the takeoff phase which is dynamic on account of the fact that the radiation emitting the electrons intermittently do so due to process constraints that are vibrational in nature and very necessary to achieve the emissions.

The sum total of the view expressed here is that the intermittent emission of electrons are the basis for the production of waves. Consequent on this observation, the electric and magnetic field amplitudes E_R and B_R in addition to the phase $\emptyset_R$ direction and its vector are crucial process conditionalities necessary for the emission of electron and other associated particles. The position of this paper is that these conditions thus obstructs undulator efficiency, with respect to the efficacy of electron mobility and the extent of photographic imaging of the target by the emitted electron.

IV. Mechanics of Thermal Conductivity and Propagating Wave Production

It should be pointed that the one-electron space analysis for photographic imaging of contact surfaces under scale up manufacturing conditions consists of a thermal conductivity ρ component whose relevance in the emission of energy in the form of wave is characteristically inter twinned with its electrical conductivity ρ_e [10] and approximately related by the expression;[11, 12]

$$\rho/\rho_e T = K = Constant \tag{12}$$

Where K represents the *Lorenz number*, which is about 22.29×10^{-9} volts^2 (^{o}K)$^{-2}$. It has been further observed that for most pure metals, this value holds or apply at 0^oC. [10]

In view of the foregoing, it should be stated that under electron scan microscopy conditions, the thermal conductivity of the metals which determine their capability to emit electrons are dependent on their collisionless conditions, as shall be discussed subsequently. The consequence of this transport phenomena is critical to the understanding of the electronic imaging photography, which is the focus of this investigation.

It is important to note that the stream of emitted electrons from where our single electron was isolated are defined by the collisionless *Boltzmann* or *Vlasov* equation,

$$\frac{D\psi(r,v,t)}{Dt} = 0 \tag{13}$$

where *D/Dt* defines the displacement derivate of the electron as an emitted particle, on a trajectory from a heated surface. Assume that our sample single electron is an integral component of an electron distribution function $\Psi(r,v,t)$.[12] As could be seen in Fig 4 below, the structural orientation of the p_x orbital is indicative of the volume element *drdv* in a *6-D directional* view.
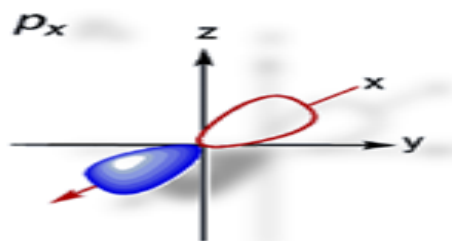
Fig 4: shape and structural orientation of *px*orbital illustrating photographic imaging syntax in x-axis. Adapted with modifications from University of Liverpool Chemtube Structural Illustration Series. Available at: www.chemtube3d.com, visited 3/3/2018

Consider that our sample electron whose p_x-*orbital* orientation as shown in Fig 4: above, occupies a position defined by a volume element *drdv* which is contained in a six-dimensional position with directional velocity space, where $\Psi(r,v,t).drdv$ accounts for total number of electrons possibly contained within the range of *r* to *r+dr* and *v* to *v+dv*. It should be noted that in the absence of any form of collision, the emitted electrons experiences external electromagnetic fields produced by a polarized ionic mass, given that the atoms having lost their valence electrons becomes positively changed ions and capable of generating wave like magnetic influence on its immediate surrounding.[13]

Further, it has been reported that [14] another source of propagating wave arises, where upon acquisition of fission energy from external sources, electrons under the excitation force are excited to the point of migration from the conduction band to the valence band. This move imply that the electron in leaving its position in the conduction band emit light, which this study observes is a partial conversion of the binding energy into light. This is akin to scratching a match stick on the rough surface of the match box. Thus, in this case energy is applied to break the bonds of the chemical deposit on the match stick, the result is binding energy conversion to heat and light energy.

V. Methods and Mono-Electron Photographic Image Acquisition Simulation

From the optical trajectory experimental simulation depicted in Fig 5 below, it would be noticed that at point AA[1] a metal of aggregate lattice bond structure receives excitation energy ΔH from a direct heating agent which was allowed to operate during the period of the investigation.'
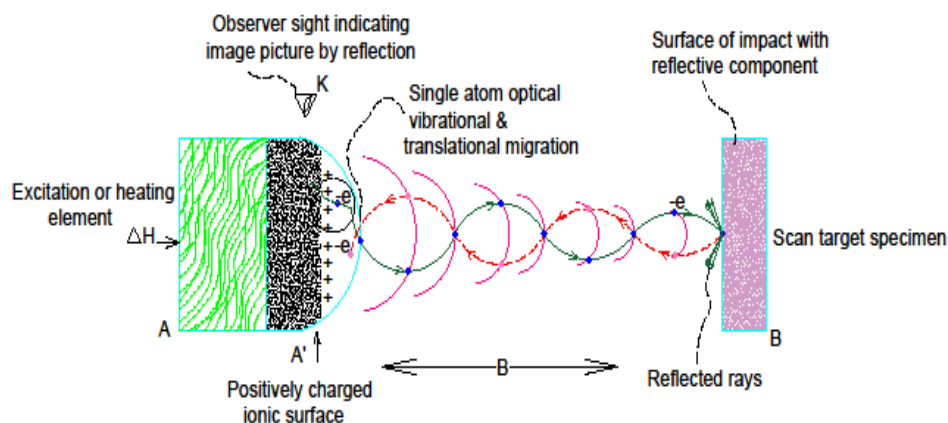
Fig 5: experimental evaluation of single electron migration and trajectory from conduction band through valence band into electromagnetic field and impact at target B

In Fig 5 we show a mono-electron migration trajectory based on acquisition of energy from point AA[1] of a high temperature metal block specimen producing a polarized ionic mass surface which produces wavelike magnetic sequence. It should be noted that this experimental evaluation of single electron migration from conduction band, through valence band into an electro-magnetic field is a definitive process for photographic image acquisition. The propagated electromagnetic field comply with all principles of wave propagation and conducts the electron away from the charged surface. The electron as a blue dot is conveyed in a wavelike motion along the green sequence indicated by forward moving arrows.

Thus, the electron maintains its spin orientation in its mean position in an energy saving vibrational manner. It is further noted that this wavelike electron trajectory terminate at the point of the scan target specimen where the electron loses some of its mobility force in the form of light energy and the rest as heat energy, which sometimes is negligible in laser scan situations. It should further be noted that upon making the impacting contact with specimen B, the electron captures the a photographic image of the target specimen and it is noticed to follow a reverse wavelike trajectory indicated by a thick purple line as a red dot back to the valence band where it recombines at the ionic surface. Discreetly, a nano-scopic observer at point K would notice that further energy is lost at the point of process recombination at the charged ionic surface.

The implication of this view is that the electron further loses energy at the point of recombination and this loss of energy is the acquired image imparting or communicating process. Thus, under nanoscale image acquisition and interpretation for in-process manufacturing quality control, this mono-electron condition is a critical necessity for analysis of material surface integrity.

In view of the foregoing, it should be noted that the work function Ø is equivalent to the electron voltage eV required to harvest an electron from the heated surface of A[1] under the condition that;

$$hf = \emptyset + E_{KE} \qquad\qquad (14)$$

where, h = the Plank's constant given as 6.63 x 10^{-34} JS
  f = frequency of the heating function in hertz (H_z)
  Ø = work function in Joules (J)
  E_{KE} = maximum kinetic energy of the emitted electron in joules (J)

The implication of equation (14) to the process is that if the heating function does not possess enough frequency by means of high intensity, there would not be enough photon to supply the required energy that would overcome the work function for the emission of the electron. Further, equation (14) can be used to indicate that the maximum kinetic energy E_{KE} if plotted against frequency f would result vibrational connotations. Thus, an increase in heating intensity also increases the frequency of vibration energy imparted on the electron to a threshold frequency f_o along the frequency axis. As indicated in Figure 4 below, an increase in frequency beyond the threshold frequency f_o also induces the maximum kinetic energy E_{KE}.
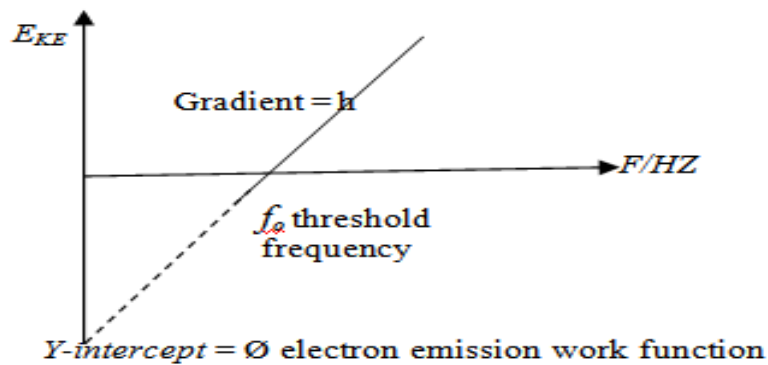
Fig 6: Graph of kinetic energy v. frequency

Further a derivative consequence of Fig 5 is the crucial factor of opto-electro-mechanical dynamics of process parameter interactions and variability on the imposition of Fig 6 significances as the forcing function required. In such a case, when E_{KE} impacts on AA[1] and the surface A[1] responds to the heating function by the emission of valence electrons. It would be noticed that surface A[1] contains ions that have lost their valence electrons. Theoretically, the ions are positively charged and constitute a cloud of positively charged particles with holes in the orbital cloud from where the electrons migrate to a higher energy level due to the excitation energy (eV).

The essence of these holes is the phenomenal *electron- hole recombination* possibilities.[15] Thus, surface A[1] is positively charged, therefore creating a positively charged electrical field and the rise in

temperature creates a spring-like restoring vibrational mechanism resulting from expansion and contraction. This internal lattice activities rise in ΔH is akin to exerting pressure on a spring and removing the pressure repeatedly.

VI. Findings and Discussion

From the foregoing it should be pointed out that the dynamically mean state spring-like return or rebounce conditions of the atoms and their bonds sends out a mechanical vibration energy at intermittent intervals equivalent to the energy released on account of inter-atomic and molecular compressive and resistive forces. The effect of this spring-like restorative action on surface A^1 is the emission of intermittent vibration sequence or signals which constitute an electromagnetic field in wave form. Thus, field B is a combination of the inter-atomic vibrational displacements of the atoms and the ionic charges at A^1. Consequently, the nature of this inter-atomic intermittent vibration can further be defined in terms of interposition of de Broglie's wavelength expressed as,

$$\lambda = \frac{h}{mV} \qquad (15)$$

into the differential equation that expresses the amplitude of the mechanical vibration displacement, given as:

$$\frac{\partial^2 \psi}{\partial x^2} + \frac{\partial^2 \psi}{\partial y^2} + \frac{\partial^2 \psi}{\partial z^2} + \frac{4\pi^2}{\lambda^2} \psi = 0 \qquad (16)$$

This canonical interposition of equation (15) on equation (16) yields the Schrödinger differential equation for wave dynamics, given as;

$$\frac{\partial^2 \psi}{\partial x^2} + \frac{\partial^2 \psi}{\partial y^2} + \frac{\partial^2 \psi}{\partial z^2} + \frac{8\pi^2 m}{h^2}(E - V)\psi = 0 \qquad (17)$$

It should be pointed that equation (17) is a crucial multidimensional definition and application for modern wave mechanics and describes the process behaviour of the optical vibrational displacements encountered as a result of the heating process and its corresponding work function embedded in the emission delivery task.

As could be noticed from Fig 5, the intermittency of the atomic contraction and repulsion actions produces high and low amplitudes space displacements described as a wave by equation (17) with a defined wavelength expressed by equation (15). This implies that this intermittent mechanical vibration possesses a phase consequence defined by the function;

$$\phi = e^{2\pi i v t} \psi(x, y, z) \qquad (18)$$

Which a phase function which is based on the time interval between optical vibration displacements in a sequence or range of vibration activity. It is therefore important to state that this time interval produces the high and low amplitudes which results the waveform expressed in equation (17). This phase function Ø is therefore theoretically linked to the wave function Ψ by the relation;

$$\psi = e^{-2\pi i \phi} \qquad (19)$$

Further, equation 19 thus holds that since a de Broglie wavelength $\lambda = \frac{h}{mV}$ then it implies that two crest of a wave and its trough in between, makes a full circle as indicated by 2π of equation (18) and (19). Thus the optical vibrational displacement that is magnetic in nature comes in contact with the charged electric field, resulting an electromagnetic field which serves as a wavelike transport medium to convey the electrons to point B, the scan target.

A proper view of Fig 5 would further indicate the movement of the electron cutting across the wave phases in a well coordinated or defined sinusoidal pattern, as if a piece of floater is placed in a pool of water that is agitated to produce waves. It would be noticed that the piece of paper without the movement of the waves would remain static, and can only be transported by the waves to the destination required. In this regard, once electrons are liberated from the conduction and valence band, they vibrate only in their mean positions and do

not leave those positions but are transported by the opto-electro-mechanical waves to deliver the energy they possess at the scan target at point B.

Thus, this study view the impact at point B as an instantaneous photographic image acquisition activity; meaning that, the single electron impact at point B reliefs it of some of its kinetic energy in order to acquire the surface imagery conditions and characteristics of the target. Advanced application have capability to capture the physical and chemical properties of the target. In the view of this study, this impact completes the first stage of photographic image acquisition circle and imparts the physical characteristics and properties of the target on the electron. Colloquially, this electron impact on target B can be said to be a rubbing off incident. Further, upon impact at point B, the second stage is accomplished by means of a revers backward return of the electron to the emitting surface where the charged cloud recombination process implies a further loss of kinetic energy by reason of deposition of the acquired photographic imagery of the surface of target B for analysis and interpretation.

5.1 Analysis of Surface Impact at Point B
An analysis of the impacting force and the consequences of that force at point B is dependent on the electron transport capability and operational velocity of the opto-electromagnetic waves as expressed in the formula. [16]

$$v = \frac{1}{\sqrt{\varepsilon\mu}} = \frac{c}{\sqrt{\varepsilon\mu_r}} \tag{20}$$

where c is the speed of light in a vacuum, μ is the permeability of free space $4\pi \, x10^{-7} \, \mathrm{H/m}$, μ_r is relative magnetic permeability of air where $\mu_r = 1$ and and $\mu = \mu_r\mu_o$. The permeability of free space = 8.854 x 10^{-12} F/m and ε_r is the relative permittivity of target B. In some metals $\varepsilon_r = 1$. This imply that, $\varepsilon = \varepsilon_r\varepsilon_o$.
Thus, a stationery particle such as an electron under the influence of equation (20) would impact a force equal to its mass, m and velocity v. Thus, in the circumstance,

$$F = mv \tag{21}$$

and;

$$KE = \tfrac{1}{2}\, mv^2 \tag{22}$$

Given that the speed of the opto-electromagnetic wave is 3 x 10^8m/s which is also the speed of light; and given also that the mass of an electron is expressed as 9.109 x 10^{-31}kg. Thus, the impacting force on B is therefore assumed to be equal to the kinetic energy 9.109 x 10^{-31} (kg) x 3 10^8 (m/s) delivered by its propelling force of the opto-electromagnetic radiation traveling in the form of a wave.

It should be noted that this impact force of the electron mass on the target B also imparts a force equal to its kinetic energy $KE = \dfrac{mv^2}{2}$; implying that,

KE = ½ 9.109 x 10^{-31} x (3 x 10^8) (J) = 8.121 x 10^{-14}J

Although in classical mechanics this force is negligible to make any reasonable impact as in the case of laser emission applications; however, it is imperative to note that under nanoscale manufacturing conditions, kinetic energy of the magnitude of 8.12 x 10^{-14}J is a significant force to make a difference in surface and image acquisition and analysis. Hence, the analysis of surface impact as indicated below is crucial to understanding this phenomena. Thus, as could be seen below the electron impact energy on target B and in return target B imparts its image and characteristics on the electron as Fig 7 simulation below illustrates.
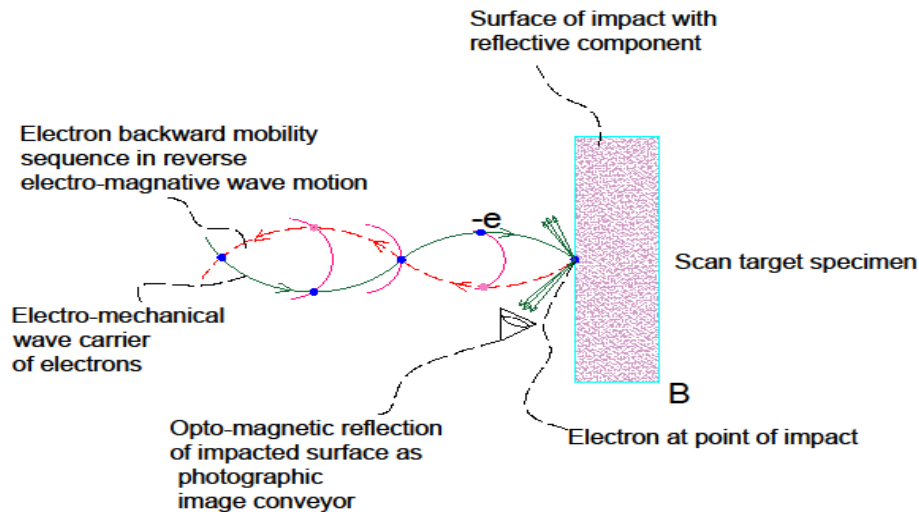
Fig 7: impact and impart diagram of electron target surface image acquisition conditions

From Fig 4 above, it could be seen that the charged electron is wave driven to make a forceful contact at target B based on the fact that from equation (22), $v = \sqrt{\dfrac{KE}{m}} = 2.985 \times 10^{22}$ m/s

In view of the foregoing postulation, the surface of the electron traveling under this speed is strong enough to capture an opto-magneto-photographic image of the impacted surface by instantaneous attraction and transfer same through opto-magnetic reflection. This process is the image scanning activity. This opto-magnetic reflection is further enhanced or sustained by a backward mobility sequence of the reversed electromagnetic wave from B to A^1. Further, the electron, *e* could be seen on a backward journey after the impact heading back to A^1 where it would meet a hole and recombine with the surface. It would further be assumed that, based on equation (13) the reverse motion of the electron would without collision follow the same wave train from the hole or associated holes back to base without interference. The implication of this view, is that should there be collisions, then the Boltzmann equation for particle distribution function Ψ (r,v,t) for gases or similar medium would apply, such that;

$$\frac{D\psi}{Dt} = \left[\frac{\partial \psi}{\partial t} \right]_{col} \qquad (23)$$

Thus, equation (23) establish the change in particle distribution with time within a confined space. The right hand side of equation (23), specifically denotes inter-particle collisions within the volume element of the phase space. Therefore the practical implication of equation (23) is that, if the reverses opto-electromagnetic wave train is subjected to the anticipations of equation (23) then photographic imagery of surface B would not be possible as the collision would have disrupted the image scan feedback process, in this regard, each electron maintain its own position in the wave train and does not collide with other electrons.

Further the electron *e* upon recombination with the orbital space previously left behind drops in energy level, and as such, acquire higher energy and moves again towards target B. The essence being to maintain the conservative law of energy and force balancing. Interestingly, at the point of recombination the electron relates or communicate the image it has acquired before obtaining further energy to proceed towards point B. It should be noted that the femtoseconds' condition of this image acquisition process makes it very difficult to microscopically determine the true nature of the process. However the case is different under nanoscale manufacturing process.

VII. Conclusion

The paper discussed Bohr's femtosecond postulation in electron energization conditions; which characteristically results the liberation of electrons from excited surfaces. This paper further utilized the gains of this electron migration from the orbital region to the conduction and valence band to show that manufacturing concerns can actually utilize this phenomenon in the areas of in-process machine vision, applicable under the automation of real-time quality assessment strategy of any *scale-up nano-manufacturing system*.

In view of the practical need to sustain the findings of this work, application of this novel technology, utilized the wriggle effect magnetic field experiment to capture the up-down and sideways undulating essence of the sinusoidal waveform that is directed at the target. In order to underscore the relevance of this machine vision enhancement effort, mono-electron computational analysis under femtosecond time frame trajectory conditionalities was deployed to resolve the electron material transportation impact within confined space which is supported by characteristic simulation experiment using SEM and graphically analyzing the sequence of the resulting trajectory based on the shape orientation of the supporting graphs.

It is therefore imperative to note that the *kinesis* of the electron is a consequential factor of the characteristics of the opto-electromechanical wave mobility; thus indicating the crucial relevance of the *photonic-phononic interplay* in the photographic image acquisition of the electron under such time constrained femtoseconds condition. Relating this consideration to the views of this study, the phonons provide the magnetic motion capability for the electron under an electron-phonon coupled [17] transport phenomenon achieved by opto-electromechanical wave dynamics. Interestingly, the photons accompany the electrons in the provision of the lighting required for the target surface image acquisition.

In view of the foregoing, the mono-electron transition condition as exemplified in this paper draws inference from the theory of dynamic wave perturbations. This imply that the mobility consequence of this wave to the delivery of atomic energy by the electron in closed coupling with a phonon is a magnetic essence directed to the acquisition of surface image of the target. The reversal trajectory in the same sinusoidal wave track is a novel ideology as the electron traces its way back to the excitation and emission point (without the consequences of Boltzmann collision function) to be relieved of the acquired image after which it is ready for further recombination and re-emission process.

Acknowledgement

References

[1]. Pellegrini, C., and Reiche, S., "The Development of X-ray Free -Electron Lasers" IEE Journal of Selected Topics in Quantum Electronics, Vol. 10 pp 1393 – 1404, 2004.
[2]. Tuma J.J., Handbook of Physical Calculations, McGraw-Hill Book Company, New York, 1976, p 173-174,
[3]. Gomis-Bresco J., Navarro-Urrios D., Oudich M., El-Jallal S., Griol A., Puerto D., Chavez E., Pennec Y., Djafari-Rouhani B., Alzina F., Martínez A., and Sotomayor Torres C. M., "A One-Dimensional Optomechanical Crystal with a Complete Phononic Band Gap", Nature Communications., Vol. 5, 4452, 2014.
[4]. Schmidt M., Kessler S., Peano V., Painter O., and Marquardt F. "Optomechanical Creation of Magnetic Fields for Photons on a Lattice" University of Erlangen-Nürnberg, Staudtstr. 7, Institute for Theoretical Physics Report, D-91058 Erlangen, Germany, p. 2, Feb, 2015
[5]. Favero, I and Karrai, K. "Optomechanics of Deformable Optical Cavities. Nat. Photonics, vol. 3, 201-205, p. 6, 2007
[6]. Tallur, S. and Bhave, S. A. A" Silicon Electromechanical Photodetector". Nano Letters, 13, 2760-2765, 2013
[7]. Pelegrini, C. "X-ray Free electron lasers and ultrafast science at the atomic and molecular scale", proceedings of EPAC 2006, Edinburg, Scotland, p. 3637, 2006
[8]. Pelegrini (EPAC 2006) at p. 3636
[9]. Pant K. K., "Free Electron Lasers, free Electron Laser Laboratory, Materials and Advanced Acceleration Sciences Division, Raja Ramanna Center for Advanced Technology (RRCAT), Indore 452013, India, pg 157.
[10]. Bird R. B., Stewat W. E., Lightfoot E. N. "Transport Phenomena", John Willey, & Sons, Inc. 1960, p. 262.
[11]. Lorenz L., Poggendorff's Annalen in Bird et al Transport Phenomena p. 262.
[12]. Wiedemann G., and Franz R. *Ann Phys. Chemie* in Bird et al – Transport Phenomena p. 262.
[13]. 13 Ross B. W., Analytical Functions and Distributions in Physics and Engineering, John Wiley & Sons Inc. London 1969 p. 415
[14]. Ohtsu M., Dressed Photons, Springer Verlag, Berlin, 2014 p.3
[15]. Ohtsu M., at p. 3
[16]. Hayt W. H., Engineering Electromagnetics 5th Ed, McGraw-Hill Pub., 1989, p. 346
[17]. Boeri, L., Calandra M., Mazin, I.I., Dolgov, L.V., Mauri, F Effects of Magnetism and Doping on the Electron-Phonon Coupling in Ba\Fe2As2., Naval Research Laboratory, Washington DC, April, 2010, p. 1 also available on the internet at www.dtic.mil/dtic/tr/fulltext/u2/a518640.pdf visited on the 20/03/2018